MEDIUM FREQUENCY RERADIATION FROM A STEEL TOWER POWER LINE WITH AND WITHOUT A DETUNER

M.A. Tilston and K.G. Balmain
Department of Electrical Engineering
University of Toronto
Toronto, Canada M5S 1A4

Abstract

Measurements and computations of field strengths and tower base currents are presented for a power line section consisting of 5 towers strung with skywires and illuminated by a nearby monopole antenna. This is done first without detuning stubs, and then with detuning stubs on one tower to reduce the re-radiation. Good agreement is obtained between moment-method computations and full-scale measurements. Computational modelling techniques to represent the power line, the detuning stubs and ground effects are given and validated. The beneficial effect of increased stub spacing from the tower leg is identified.

Introduction

An AM broadcast antenna consists of one or more towers which are fed to produce a circular or directional radiation pattern. This pattern is often required to be precisely maintained to avoid interference with other stations, and to provide adequate service. The vertically polarized medium frequency radiation from an AM broadcast antenna, when incident on a steel tower power line, will induce currents in the power line. These currents will re-radiate the AM broadcast signal and the re-radiation will add to the direct antenna radiation to either increase or decrease the broadcast signal, depending on their relative phase relationship. Thus, re-radiation can decrease the service area and increase interference levels of a broadcast station.

One way of alleviating a re-radiation problem is to add detuning stubs to the power line. These stubs will alter the induced current distribution, thereby altering the re-radiation pattern. Usually by this method the average level of re-radiation can be reduced.

In order to predict the impact on a broadcast station of having a re-radiation problem due to a power line (with or without detuners), computer modelling by moment method or physical scale modelling can be carried out. However, any modelling techniques should be validated against full scale measurements. Although many full scale measurements have been done, largely by broadcast engineers in the course of pattern adjustment, they generally include the effects of other unknown re-radiators and unknown ground conductivity variations. Because of the unknowns, these measurements are insufficient for validation of modelling techniques. Thus, carefully controlled measurements are required as part of an integrated model validation program.

Re-radiation from a Power Line Strung with Skywires

Introduction

It was desired to show the correlation between moment method computations and full scale measurements for a section of power line. Silva, Balmain and Ford [1], obtained good correlation between computed and measured effects of an operating power line on the pattern of a dual-frequency directional antenna near London, England. In the case they studied, the re-radiation was small and significantly affected only the minor lobes, leaving the main lobe relatively unperturbed. To investigate the subject further, a full scale experiment was devised to obtain measurements of a severe re-radiation problem. The approach was to set up a monopole antenna very close (256 m) to an isolated section of power line, and test at eight frequencies through the AM broadcast band. A good background for this study is provided in a paper by Tilston and Balmain [2] who studied re-radiation from an unstrung power line tower, comparing measurements with moment-method computations.

Test Site

The test site was a section of the Ontario Hydro Claireville-Cherrywood 500 kV line near Thornhill, Ontario. This was the same site used for earlier unstrung tower tests [2]. The physical arrangement shown in Figure 1 included a five-tower section of power line strung with two lightning wires (skywires) which connect to the top crossarms, but no power wires (phase conductors). The phase conductors have been shown to have negligible effects on the re-radiation due to a vertically polarized incident field [3], [4]. Because the test setup was designed to permit mounting of stubs on skywires, the skywires were supported by insulated rollers to allow lowering of a span to ground level by means of loosening the tie-down wires which sloped from the top of tower one to ground anchors. While testing, the skywires were electrically connected to the towers, and the tie-down wires were broken with insulators at each end. The monopole antenna was located 256 m from the closest point on the power line, a distance which is also approximately the intertower spacing.

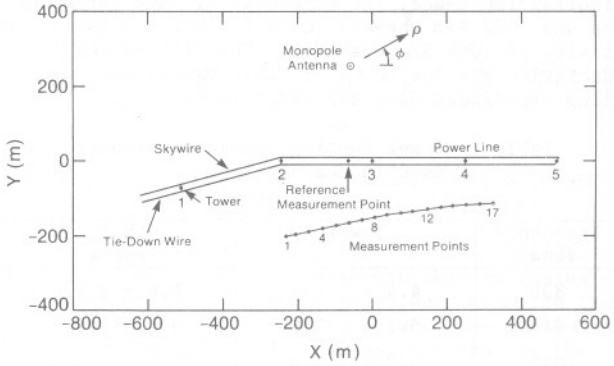

Figure 1: Test site geometry.

The measurement points were selected to be near enough to the power line that any external re-radiators, such as other nearby power line towers, low voltage lines, and buildings, would not significantly affect the measurements. The measurement point and antenna coordinates were determined with a survey transit.

The ground was flat, well-cultivated farm land, with an unusually high water table at tower three as determined by soil studies.

0018-9316/84/0300-0017$01.00©1984 IEEE

Measurements

Measurements of $|H_\phi|$ were made at seventeen points along a path approximately parallel to the power line, and one reference point under the power line at the point nearest the antenna. At the reference point, the measured $|H_\phi|$ is primarily due to the antenna, because the power line contribution is mainly H_ρ due to the site geometry.

In this paper, the quantity $|\rho H_\phi / \rho_o H_{\phi_o}|$, where the zero subscripts denote the reference point, is called the $|H_\phi|$ perturbation for the following reason. The measurement points are far enough from the omnidirectional antenna that its H_ϕ variation is inverse distance, hence the antenna $|\rho H_\phi|$ is theoretically the same for all measurement points. At the reference point, the measured $|\rho_o H_{\phi_o}|$ is primarily due to the antenna because of the geometry, so that

$$\left|\frac{\rho\ H_\phi}{\rho_o\ H_{\phi_o}}\right| \doteq \left|\frac{\rho\ H_\phi}{\text{antenna}\ \rho\ H_\phi}\right| = \left|\frac{H_\phi}{\text{antenna}\ H_\phi}\right| \qquad (1)$$

This is verified later by computation.

The perturbation patterns are smooth curves, with maximum peak-to-peak variations occurring for 830 kHz (4.7 dB) and 1200 kHz (4.3 dB). These frequencies which produces maximum perturbations are called resonant frequencies of the power line. Any contribution from distant external scatterers would appear as ripples or spikes in the patterns but because these are not apparent, such scatterers must be insignificant.

Computational Modelling of Ground Effects

Previously [2], the effect of a lossy ground on an unstrung power line tower was represented as a lumped impedance (footing impedance) between the tower base and a perfectly conducting ground. The footing impedance was computed by first representing the power line tower with its four legs and four ground anchors (footings) as an equivalent uniform pole on an equivalent footing. Monteath's compensation theorem formulation [5] was then applied to obtain the footing impedance to be used with a perfectly conducting ground. In the present study, the same approach was used to compute a footing impedance for each tower. In the computations of footing impedance, the conductivity used for tower three was .022 S/m whereas for all other towers, a conductivity of .006 S/m was used. The differences in conductivity are due to water table variations. The footing impedances used are given in Table 1.

Table 1 Tower footing impedances (ohms) used in computations

Frequency (kHz)	Tower 3	Other Towers
830	4.4 + j 2.6	8.6 + j 4.6
940	5.1 + j 2.6	9.9 + j 4.5
1030	5.7 + j 2.6	11.1 + j 4.4
1100	6.2 + j 2.5	12.1 + j 4.1
1200	7.0 + j 2.3	13.6 + j 3.6
1300	8.0 + j 2.1	15.4 + j 2.9
1400	9.1 + j 1.6	17.4 + j 1.9
1580	11.6 + j .25	22.0 - j 1.2

Based on the assumption that the skywire carries TEM waves, the compensation theorem can be used to calculate the propagation constant including ground effects as done by Knight [6] for a single horizontal wire over ground. The result is given in Appendix A, along with a simplification which allows the ground effects to be represented as an equivalent finite conductivity of the skywires over a perfectly conducting ground. The equivalent skywire conductivity σ_w is

$$\frac{\sigma_w}{\sigma_g} = \left(\frac{h}{2a}\right)^2 \qquad (2)$$

where σ_g is the actual ground conductivity. For the typical wire height of 52 m, wire radius of .00635 m, and ground conductivity of .006 S/m, the equivalent wire conductivity from equation (2) is 100 kS/m. The actual wire is aluminum strands around a steel core (ACSR) with an estimated conductivity of 36 MS/m, which is much greater than that due to ground effects. The wire conductivity used for all sky-wires, including the tie-down wires, was 100 kS/m.

The effect of finite ground conductivity on ground wave propagation from the antenna and power line to the measurement points was neglected.

Simulation

In the unstrung tower study of tower three [2], a "T" model for the power line tower was developed which consisted of a constant-radius vertical member and a constant-radius horizontal member. Computations of re-radiation using the Numerical Electromagnetics Code moment method (NEC) [7] showed the T model to be approximately equivalent to a detailed model. The crossarm radius of the T model was changed to 0.3 m to improve the agreement with the detailed model. This T model was used in the present study to represent tower three with skywires attached. Because the other four towers were similar in shape to tower three, the T model derived for tower three was used for the other towers, with only the height adjusted to match the actual tower height which ranged from 51 to 55 m. The two skywires were modelled as straight wires with no sag, spaced 21.4 m apart. The tie-down wire insulators were modelled as air gaps, that is, the wires were broken at the ground and at the top of tower one so that no direct electrical connection existed. The power line model is depicted in Figure 2 which shows the ninety-five segments used along with their dimensions. The antenna model is a three-segment uniform pole, 29 m high and 0.042 m in radius, which was developed in the unstrung tower simulation [2]. As detailed in the previous section, ground effects were represented in the model by lumped tower footing impedances, equivalent skywire conductivity, and a perfectly conducting ground plane.

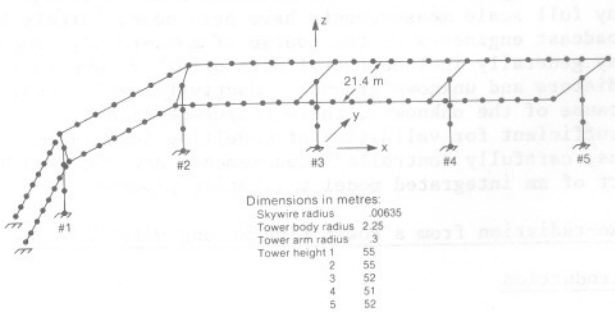

Figure 2: Sketch of power line model used for NEC computations, showing segment junctions and endpoints as dots.

The NEC program was used to compute H_ϕ at the measurement points on the eight measurement frequencies.

Plotted in Figure 3 are the corresponding $|H_\phi|$ perturbation values $|\rho H_\phi / \rho_o H_{\phi_o}|$ for both computations and

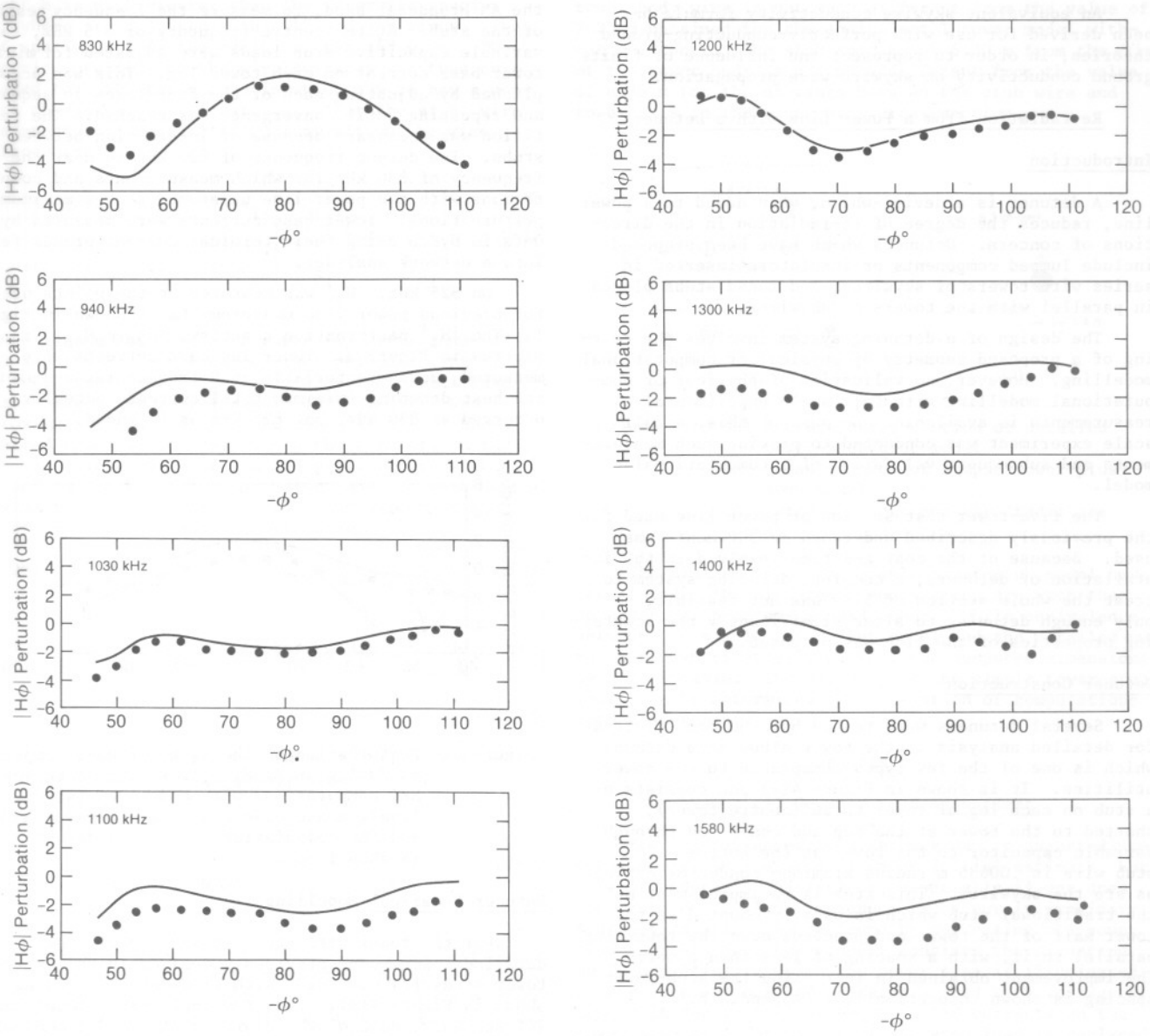

Figure 3: Perturbation of the H_ϕ magnitude, computed as 20 $\log|\rho H_\phi / \rho_o H_{\phi_o}|$, versus azimuth for both NEC computations (solid line) and measurements (circles) at the eight frequencies indicated.

measurements. To prove that this quantity is indeed a perturbation, computations were done including only the antenna contribution to H_ϕ, and the resulting values of $|\rho H_\phi / \rho_o H_{\phi_o}|$ were within the range of -0.2 to 0 dB. From the $|H_\phi|$ perturbation patterns, it can be seen that the shape of the curves is well predicted by the computational model, but the computed level varies from close correspondence to as much as 2 dB higher than measurements in some cases. The computed perturbation level seems to be correct at the resonant frequencies of 830 kHz and 1200 kHz. Because the pattern shape is well predicted, the computed currents on the power line relative to the antenna must be correct, so that the computed far field pattern should be reliable in terms of shape, with some uncertainty about level. The problem with level does not appear to be related to frequency or the degree of resonance, and is likely due to variable error in calibration of the field strength meter used for measurements.

One method of saving computer memory in power line analysis is to represent the two skywires as one thicker skywire connected to the tops of the tower bodies. This was done on NEC using an equivalent skywire radius of 0.37 m, computed using the cage antenna equation from Schelkunoff [8]. The resultant power line model required only 60 segments instead of 95 as required for the two-skywire model. Perturbation patterns were again calculated using NEC and the values obtained deviated a maximum of .7 dB and typically .2 dB from two-skywire model computations.

Summary

Computer modelling of a five-tower power line section has produced $|H_\phi|$ perturbation patterns which agree well with measurements in terms of shape but have up to a 2 dB higher level. The level discrepancy could be due to measurement calibration error.

Because the computed near field pattern shape is accurate, then the computed far field pattern shape

should be accurate also.

To save computer memory, the equivalent single skywire model can be used without serious error.

An equivalent skywire conductivity formula has been derived for use with perfectly-conducting-ground theories, in order to represent the influence of finite ground conductivity on skywire wave propagation.

Re-radiation from a Power Line with a Detuner

Introduction

A detuner is a device which, when added to a power line, reduces the degree of re-radiation in the directions of concern. Detuners which have been proposed include lumped components or insulators inserted in series with towers or skywires, and tuned stubs placed in parallel with the towers or skywires.

The design of a detuning system involves the testing of a proposed geometry by physical or computational modelling. However, no validation of physical or computational modelling with full scale experimental measurements is available. Because of this, a full scale experiment was conducted to provide such measurements and subsequent validation of a computational model.

The five-tower test section of power line used for the previously described undetuned measurements was used. Because of the cost and time involved in the installation of detuners, a complete detuning system to treat the whole section of line was not feasible, so only enough detuning to alter significantly the scattering properties of the line was proposed.

Detuner Construction

Several detuners were tested but the one selected for detailed analysis is the tower elbow stub detuner which is one of the few types acceptable to the power utilities. It is shown in Figure 4(a) and consists of a stub on each leg of tower three (centre tower), shorted to the tower at the top and connected through a variable capacitor to the tower at the bottom. The stub wire is .00635 m radius aluminum conductor cable, as are the skywires. This stub is an improvement on the traditional stub which is usually mounted on the lower half of the tower and proceeds down the tower leg parallel to it, with a spacing of less than a metre. The improvement obtained in incr sing the stub-tower spacing is shown theoretically i Appendix B.

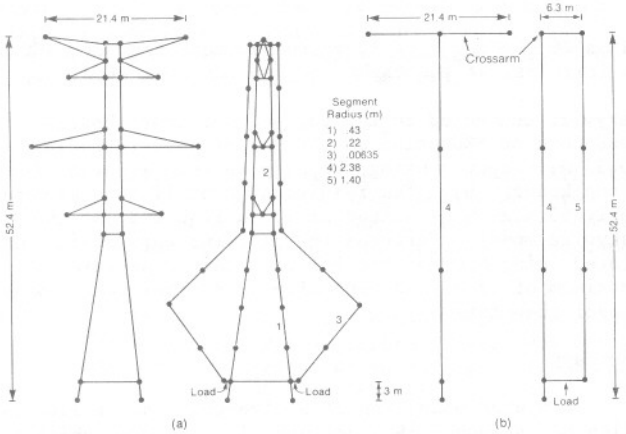

Figure 4: Front and side views of tower-plus-stub models used for NEC computations:
(a) detailed model with elbow stub;
(b) equivalent simple model with parallel stub.
Dots show segment junctions and endpoints.
Some segment radii are shown.

Measurements

It was decided to work with transmitter frequencies from 795 kHz to 855 kHz, which was a quiet section of the AM broadcast band, to measure the frequency response of the stub. At the centre frequency of 825 kHz, the variable capacitive stub loads were adjusted for minimum tower base current on each tower leg. This was accomplished by adjusting each of the four loads in sequence, and repeating until convergence was reached. The repetition was necessary because of interaction between stubs. The detune frequency of 825 kHz is near the frequency of 830 kHz for which measurements and computations with the power line undetuned showed maximum perturbations. Tower base currents were measured by Ontario Hydro using their toroidal current probes fed into a network analyser.

On 825 kHz, $|H_\phi|$ was measured at the points used for previous power line measurements as shown in Figure 1. The $|H_\phi|$ perturbation quantity, $|\rho H_\phi / \rho_o H_{\phi o}|$, is plotted in Figure 5. Tower leg base currents were measured, added vectorially on 9 frequencies and plotted: the best detuning (minimum total current) actually occurred at 830 kHz, not 825 kHz as intended.

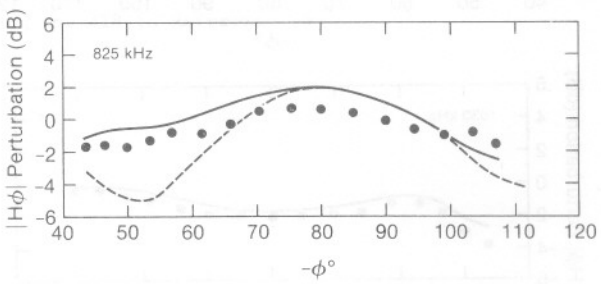

Figure 5: Perturbation of the H_ϕ magnitude, computed as 20 $\log|\rho H_\phi / \rho_o H_{\phi o}|$, versus azimuth for NEC computations with a detuner (solid line), measurements with a detuner (circles), and NEC computations without a detuner (dashed line).

Detuner Numerical Modelling

For the tower with stubs (tower three), the detailed tower model previously derived in the unstrung tower study [2] was used, with elbow stubs added as shown in Figure 4(a). This tower-plus-stub model has 144 segments, some of which are located and dimensioned such that numerical errors in computation may occur. One such problem is the short wire segment joining the top of the stub to the tower. This segment is only .0025λ at 825 kHz which approaches the recommended minimum segment length in NEC of .001λ. Also, there is a large change in radius between this segment and the tower leg to which it is joined. The ratio of radii between the stub and the tower leg at the top connection point is 35 and at the bottom connection point is 68. The relevant specification in NEC says that there should not be a large difference in the radii of adjoining segments, but no specific number is given. Furthermore, past experience has shown that errors can result when parallel wires are spaced less than .01λ, especially when the currents are nearly equal in magnitude but in antiphase. The spacing between the stub wire and tower leg on the upper half of the tower is .00248λ at 825 kHz, which is less than the minimum reliable spacing of .01λ. For these reasons, the model was tested for numerical errors. To test the model tower-plus-stub, an incident plane wave was used, and the capacitive loads were numerically adjusted on NEC to be equal and to produce a minimum total base current at 830 kHz. The base current was reduced by 13 dB over the undetuned compu-

tations at 830 kHz, but when the frequency response of the current was investigated, it was erratic and the degree of detuning near 830 kHz was typically only 3 dB. Thus it was decided that this model was not acceptable for studying frequency response.

It was thought that an equivalent simple tower-plus-stub model might be derived using a T tower model with a single parallel stub as shown in Figure 4(b). The crossarm dimensions and height were chosen to be equal to those used for the T tower model without a detuner. The parameters remaining to be found were the tower body radius, stub radius and tower-stub spacing. The procedure for determining these parameters, as detailed in Appendix C, was to find the average spacings and radii of the tower legs and stubs on the detailed tower-plus-stub model. Then, considering infinitely long wires with these cross-sectional dimensions parallel to a distant ground plane, the static solution for the electric potential on the wire surfaces was obtained. In this calculation, it was assumed that the four tower legs had equal charges per unit length, and the four stub wires also had equal charges per unit length. This symmetry was approximately true in the computations with the detailed tower-plus-stub model which had equal stub loads and yielded currents generally within ±5% and ±7° of each other on symmetric wires. If the stub loads had been much different, the symmetry would not exist. Next, the electric potential on the wire surfaces in the equivalent single-wire tower and single-wire stub were calculated and equated to those of the four-wire tower, four-wire stub configuration. The resulting dimensions for the equivalent tower-plus-stub model are such that the single-wire tower radius equals the geometric mean of the four-wire leg spacings, including the self spacing or radius, and such that the single-wire stub radius equals the geometric mean of the four-wire stub spacings including the self spacing or radius. The equivalent tower-stub spacing equals the geometric mean of the spacing between one of the four stub wires and the four tower legs. The average cross-sectional dimensions for the detailed tower-plus-stub model were found to be .35 m and .00635 m for the tower leg and stub radii, with the tower legs forming a square cross-section of width 4.02 m and the stub wires forming a rectangular cross-section of width 4.02 m and length 11.9 m. After calculation of the specified geometric means, the equivalent simple tower-plus-stub model has a tower radius of 2.38 m, a stub radius of 1.4 m, and a tower-stub spacing of 6.30 m. These dimensions do not result in any of the numerical instability problems mentioned earlier in connection with the detailed model.

With the simple tower-plus-stub model shown in Figure 4(b), the stub capacitive load was adjusted numerically on NEC to minimize the tower base current for plane wave incidence at 830 kHz as was done previously for the detailed model, and the frequency response was studied. The base current at 830 kHz was reduced by 49 dB over that computed without a detuner. The frequency response was smooth and showed no signs of numerical instability. Therefore the simple tower-plus-stub model was considered to be reliable for use in a complete power line model.

Simulation

The H_ϕ was computed on NEC for the power line model which uses the T tower model with two skywires as in Figure 2, but with the simple tower-plus-stub model for tower three. The detuner capacitive load was adjusted numerically to minimize the tower base current at 830 kHz, the frequency at which the measured current was minimum. The detuner load could have been adjusted by iteration, but a more efficient approach was used, as detailed in Appendix D. The procedure is based upon the fact that the current on a power line with one load can be expressed as a sum of two modes which can be computed on NEC. The first mode is obtained by shorting the load and applying the antenna voltage source, and the second mode is obtained by turning off the antenna source and applying a voltage source of arbitrary strength in place of the load. The coefficient of the second mode is chosen to produce a total current of zero at the base of tower three. The total voltage and current at the load location then specify the load impedance. The impedance contains a small resistance and large reactance. The resistance can be omitted from the load and can still yield good detuning. In the specific model under study, detuned at 830 kHz, the optimum load impedance obtained was 4.5-j 324 ohms. The load used for computations was a capacitance of 592 pF, corresponding to -j 324 ohms at 830 kHz. With this load value, the tower three base current was reduced by 28 dB over that for the computations without detuning.

The H_ϕ was computed on NEC for 825 kHz at the measurement points and the $|H_\phi|$ perturbation, $|\rho H_\phi / \rho_o H_{\phi o}|$, was plotted along with the measurements on Figure 5. Also shown, as a dashed line, are computations for the undetuned power line. It can be seen that for the detuned power line, the computations produce a curve similar in shape to the measurements, but typically 1.5 dB higher in level. This means that the computed power line currents must be correct relative to the antenna current, so far field computations should be reliable for pattern shape, with some uncertainty about level. The discrepancy in level may be attributed to error in calibration of the field strength meter used for measurements. It should be noted that the computed detuned curve is quite different from the undetuned curve and that the detuned measurements correlate well with the detuned computations and poorly with the undetuned computations. The far E_θ for θ=90° was computed and plotted in Figure 6 for the power line with and without a detuner, and for the antenna alone. It shows that even though only one tower was detuned, the maximum far field perturbation was reduced from 4.5 dB to 2.4 dB.

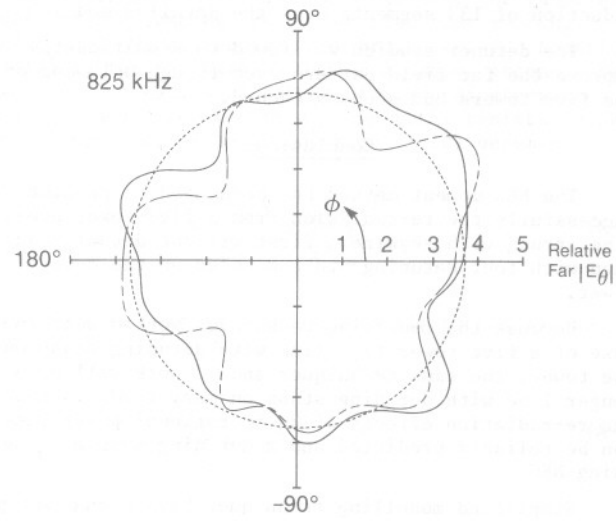

Figure 6: Polar pattern at θ=90° of relative far $|E_\theta|$ on a linear scale, for NEC computations of the power line with a detuner (—), without a detuner (— - - —), and antenna alone (---).

The frequency response of the stub was studied by computing the tower base current over the frequency band of 795 kHz to 855 kHz. The computations are plotted in Figure 7 along with the sum of the measured currents on the four tower legs. The difference between computations and measurements is typically 3 dB which is good considering that the computed reduction in

current produced at the detune frequency was 28 dB. Furthermore, the correlation can be greatly improved by shifting the computed curve up in frequency by 4 kHz, which could be done by numerically readjusting the load. It may be that the current measured at 830 kHz was a false minimum caused by instrumentation error, and that the true minimum should have been found at 834 kHz. Overall, the computational model appears to give reasonable agreement with the measurements for level and frequency response of the detuned tower base current.

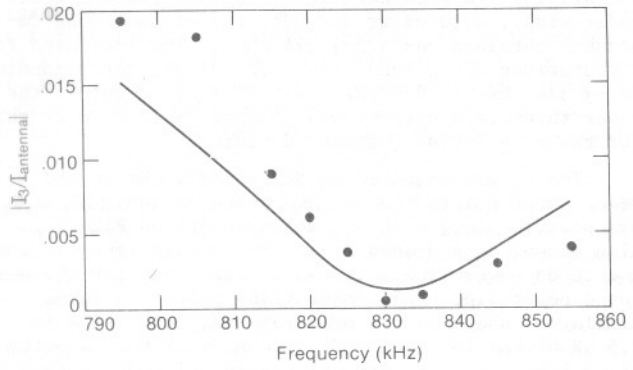

Figure 7: Total base current of tower 3 (normalized by antenna input current) versus frequency, with a detuner on tower 3. The solid line is from NEC computations, and the circles are measurements.

Summary

The detuner characteristics were found to be well predicted by NEC with some modelling precautions to avoid numerical errors. The precautions necessitated developing a simplified model of the tower-plus-stub combination. This simplified model also provided a reduction of 133 segments over the detailed model.

The detuner studied was found to significantly improve the far field pattern even though only one of the five towers had stubs attached.

Conclusions

The NEC moment method has been used to predict successfully the re-radiation from a five-tower power line strung with skywires, first without detuning and then with four detuning stubs mounted on the centre tower.

Because the modelling techniques worked well in the case of a five tower test line with detuning stubs on one tower, the same techniques should work well on a longer line with detuning stubs on many towers. Hence, the re-radiation effects of an operational power line can be reliably predicted and a detuning system designed using NEC.

Simplified modelling techniques have been developed to obtain tower and stub models with reduced numbers of segments, and to eliminate numerical instability. Ground effects have been modelled using equivalent tower footing impedances and equivalent skywire conductivity: these representations for ground effects were necessary to produce agreement between theory and full-scale experiments.

The elbow stub for towers is theoretically a significant improvement in terms of load sensitivity over the traditional close-spaced parallel stub, and has been found to be practical to construct and adjust.

The field strength measurements, which were all near the power line, show none of the signs of unknown variable ground wave attenuation or re-radiation from external sources which have been evident in many of the far field measurements done in the past. Thus, the preferred location for obtaining measurements to correlate with computations is near the power line.

In summary, the degree of success of the computational method presented here in correlating with the measurements warrants its use in designing a complete detuning system for an operational power line.

Appendix A

Skywire-Ground Interaction

Although the skywires are at a height of slightly over a quarter wavelength at the highest frequency of 1580 kHz, they can still be assumed to carry mainly a TEM or transmission line mode. Knight [6] computed the effect of a lossy ground on the propagation constant of a TEM wave on a wire over ground using Monteath's compensation theorem [5]. Knight's expression for the propagation constant γ, in terms of the propagation constant γ_o and the transmission line characteristic impedance Z_o for a wire over a perfectly conducting earth, with wire height h, and ground surface impedance η_g, is

$$\gamma = \gamma_o \left(1 + \frac{\eta_g}{2\pi h Z_o \gamma_o}\right)^{\frac{1}{2}} \quad . \qquad \text{(A-1)}$$

The ground surface impedance for a homogeneous earth of conductivity σ_g, relative permittivity ε_r, and a free space wavelength of λ_o, is

$$\eta_g = 120\pi/(\varepsilon_r - j60\sigma_g\lambda_o)^{\frac{1}{2}} \quad . \qquad \text{(A-2)}$$

The characteristic impedance of a wire of radius a, over a perfectly conducting ground plane, is

$$Z_o = 60\ \ell n\ (2h/a) \qquad \text{(A-3)}$$

and the propagation constant γ_o, of a perfectly conducting wire over a perfectly conducting ground plane is

$$\gamma_o = j\ 2\pi/\lambda_o \quad . \qquad \text{(A-4)}$$

In using the equation (A-3) for two skywires, their equivalent single wire radius should be used, obtained using the cage antenna equation from Schelkunoff [8]. This yields an equivalent radius equal to the geometric mean of the actual (two-wire) skywire radius and spacing.

With the given geometry and electrical constants, considerable simplification of equation (A-1) is possible. Typical parameters are h = 52 m, a = .37 m (actual skywire radius of .00635 m and spacing of 21.4 m), ε_r= 15, and σ_g = .006 S/m. They result in values of Z_o= 338 ohms, $|\eta_g|$ ranging from 33 to 46 and $|\gamma_o|$ ranging from .017 to .033 for frequencies ranging from 830 kHz to 1580 kHz. Thus the second term in the parentheses of equation (A-1) is much less than one (<.018) and the equation can be approximated as

$$\gamma = \gamma_o \left(1 + \frac{\eta_g}{4\pi h Z_o \gamma_o}\right) \quad . \qquad \text{(A-5)}$$

Also, in the equation for η_g, $60\sigma\lambda_o >> \varepsilon_r$ and η_g can be approximated as

$$\eta_g = 120\pi/(-j60\sigma_g\lambda_o)^{\frac{1}{2}}$$

$$= (1+j)120\pi/(120\sigma_g\lambda_o)^{\frac{1}{2}} \quad \text{(A-6)}$$

Placing equation (A-6) in (A-5), with $\gamma_o = j\frac{2\pi}{\lambda_o}$ yields

$$\gamma = \alpha(1+j) + \gamma_o \quad \text{(A-7)}$$

where

$$\alpha = \frac{30}{hZ_o(120\sigma_g\lambda_o)^{\frac{1}{2}}} \quad \text{(A-8)}$$

In the imaginary terms of γ, the first term (α) is always less than 0.61% of the second term so that the wavelength is approximately the same for lossy ground as for perfectly conducting ground.

Now consider a wire of finite conductivity σ_w over a perfect ground plane. If the wire skin depth is much less than its radius, its surface impedance Z_s will be approximately equal to that of a flat conductor of the same material, given as [9]

$$Z_s = \left(\frac{\omega\mu}{2\sigma_w}\right)^{\frac{1}{2}}(1+j) \quad \text{(A-9)}$$

and the impedance per unit length z is then

$$z = \frac{1}{2\pi a}\left(\frac{\omega\mu}{2\sigma_w}\right)^{\frac{1}{2}}(1+j)$$

$$= r(1+j) \quad \text{(A-10)}$$

where r is the resistance per unit length. The propagation constant for a transmission line is [10]

$$\gamma = [(R+j\omega L)(G+j\omega C)]^{\frac{1}{2}} \quad \text{(A-11)}$$

where in this case,

$$\begin{aligned} R &= r \\ j\omega L &= jr + j\omega L_o \\ j\omega C &= j\omega C_o \\ G &= 0 \end{aligned} \quad \text{(A-12)}$$

and the zero subscript denotes values for a zero surface impedance wire. After substitution of equations (A-12) into (A-11), we have

$$\gamma = [(r + jr + j\omega L_o)(j\omega C_o)]^{\frac{1}{2}}$$

$$= j\omega(L_oC_o)^{\frac{1}{2}}\left[1+\frac{r}{j\omega L_o}(1+j)\right]^{\frac{1}{2}} \quad \text{(A-13)}$$

If $r \ll \omega L_o$ (as will be verified later), then

$$\gamma = j\omega(L_oC_o)^{\frac{1}{2}}\left[1+\frac{r}{2j\omega L_o}(1+j)\right]$$

$$= \frac{r}{2}\left(\frac{C_o}{L_o}\right)^{\frac{1}{2}}(1+j) + j\omega(L_oC_o)^{\frac{1}{2}} \quad \text{(A-14)}$$

which reduces to

$$\gamma = \frac{r}{2Z_o}(1+j) + \gamma_o \quad \text{(A-15)}$$

For this lossy wire over perfect ground to be equivalent to the perfectly conducting wire over lossy ground, the propagation constants must be equated in (A-15) and (A-7) with the result,

$$\frac{r}{2Z_o} = \alpha \quad \text{(A-16)}$$

or from (A-8) and (A-10),

$$\frac{1}{4\pi aZ_o}\left(\frac{\omega\mu}{2\sigma_w}\right)^{\frac{1}{2}} = \frac{30}{hZ_o(120\sigma_g\lambda_o)^{\frac{1}{2}}}$$

which simplifies to

$$\frac{\sigma_w}{\sigma_g} = \left(\frac{h}{a}\right)^2 \quad \text{(A-17)}$$

Using equations (A-16) and (A-8) to find the range of r over the frequencies tested, we find that $r \ll \omega L_o$ ($r/\omega L_o \leq .016$), as required to obtain (A-14). Equation (A-17) is for one wire of radius a, above ground. For two wires of radius a' with equivalent single-wire radius a and conductivity σ_w', the total resistance per unit length, r, given in equation (A-10) becomes

$$r = \frac{1}{2\pi 2a'}\left(\frac{\omega\mu}{2\sigma_w'}\right)^{\frac{1}{2}} \quad \text{(A-18)}$$

When this is used in equations (A-12) to (A-17), we obtain

$$\frac{\sigma_w'}{\sigma_g} = \left(\frac{h}{2a'}\right)^2 \quad \text{(A-19)}$$

This specifies the wire conductivity to be used for two skywires over a perfectly conducting ground plane, to represent the effect of a lossy ground on perfectly conducting skywires. Substitution of the actual skywire values of h = 52 m, a = .00635 m and σ_g = .006 S/m results in an equivalent wire conductivity of 100 kS/m to represent ground effects.

The actual skywires are made of .00635 m radius stranded aluminum cable with a steel core, referred to as ACSR cable. The conductivity for aluminum is approximately 36 MS/m, and is thus insignificant compared to the equivalent wire conductivity of 100 kS/m required to represent ground effects.

Appendix B

Theoretical Comparison of Detuning Stubs for an Isolated Power Line Tower

The effect of spacing of detuning stubs from the tower legs was investigated theoretically using NEC. The detailed tower model in Figure 8(a), which represents a 52.4 m high 500 kV type V1S power line tower, was used as a basis for the tower-plus-stub model in Figure 8(b) which has more tower lattice members in the stub vicinity, but omits the two shortest pairs of crossarms to conserve computer memory. The stubs tested were made of .00635 m radius perfectly conducting wire, occupying the lower half of the tower. Each of the four tower legs had a stub connected to it. The bottom of the stub contained a capacitive load in series with it. Three different stub types were tested, a parallel stub spaced 1 m from the tower leg, a parallel stub spaced 3 m from the tower leg, and an elbow stub with a tower spacing of 3 m at the top and bottom, and 13 m at the midpoint. Computations on NEC were done for the re-radiated far field due to a plane wave at 860 kHz incident on the model tower, first without stubs and then with a stub on each leg, for each of the three stub types considered. For each stub type, the capacitive load reactance was varied from zero to infinity. The resulting re-radiated far E_θ at $\theta=90°$ for the elbow stub is plotted in Figure 9(a). It shows that at the detuned load value, the re-radiation is greatly suppressed by more than 25 dB over the undetuned value, while an increase in load reactance of 25% maximizes the re-radiation, an increase of 13 dB over the undetuned value. Also, a zero load reactance results in almost the same re-radiation as the undetuned tower, while an infinite load reactance increases the re-radiation by 1.7 dB.

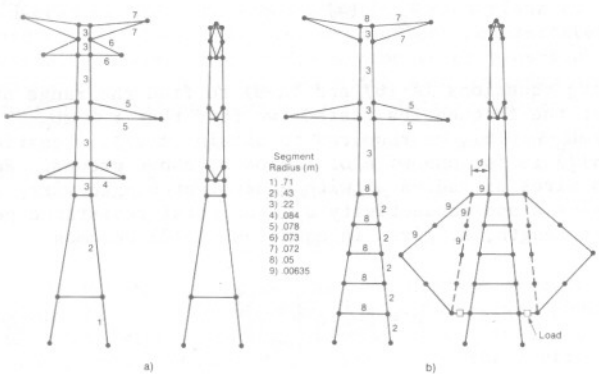

Figure 8: Front and side view of models for NEC computations showing segmentation and wire radii. (a) Model for tower without stubs. (b) Model for tower with loaded stubs of three types: (1) elbow stub (solid line); parallel stub (dashed line) with (2) d = 3 m, and (3) d = 1 m.

To compare stub types, the re-radiation sensitivity to load variation was studied near the detuned load values. Figure 9(b) shows the re-radiated far E_θ at $\theta=90°$ versus load reactance for the three stub types. It is evident that as the load is varied away from the detuned value, the re-radiation increases least for the elbow stub. This means that for a given degree of detuning, the elbow stub allows a greater tolerance in load reactance for both initial adjustment, and long term drift.

The beneficial effect of the elbow stub is probably due to its larger spacing from the tower rather than its shape, just as the parallel stub with 3 m spacing was an improvement over the parallel stub with 1 m spacing. The advantage of the elbow shape over the parallel geometry is that the elbow can be constructed using an insulated guy wire slanting from the elbow midpoint away from the tower, and down to the ground.

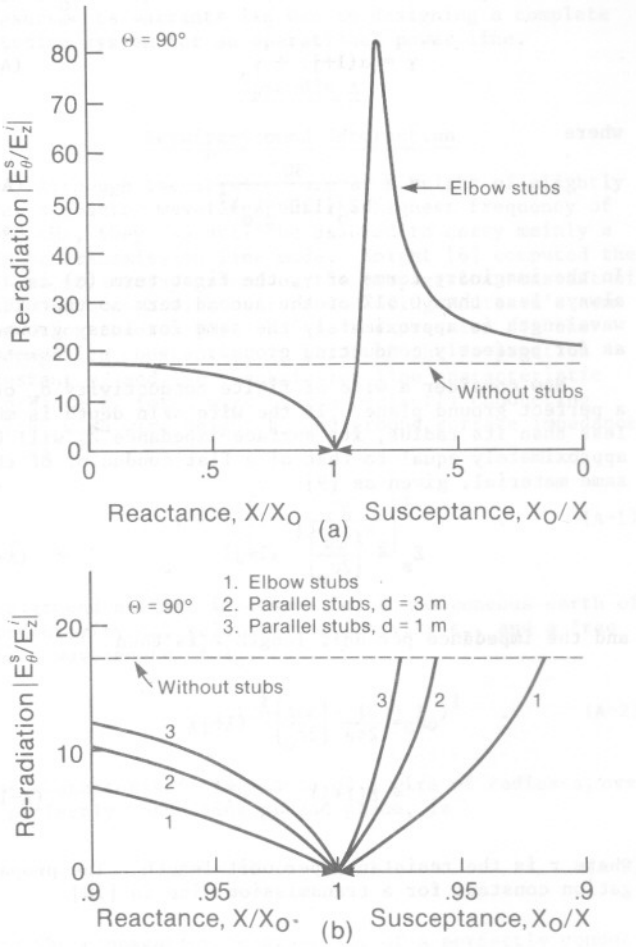

Figure 9: Re-radiated far field from a tower with a loaded stub versus stub load. The re-radiated field (E^s_θ) is normalized by the incident field (E^i_θ).
(a) Response with elbow stubs for full load variations.
(b) Comparison of stubs near optimum detuning.

Appendix C

Equivalent Tower-Plus-Stub Model

A simple tower-plus-stub model was desired which would consist of one wire to represent the tower body and one wire parallel to it to represent the stub as shown in Figure 4(b). The tower crossarms were represented by one pair of crossarms at the tower top with the same dimensions used for the simple T model of a tower without a detuner. The average tower leg and stub wire spacings and radii, of the detailed tower-plus-stub model shown in Figure 4(a), were calculated. This average cross-section is given in Figure 10(a) and consists of eight wires, including four tower legs of radius .35 m forming a square of width 4.02 m, and four stub wires of radius .00635 m forming a rectangle of width 4.02 m and length 11.9 m. To obtain the desired two-wire cross-section of Figure 10(b) from the eight-

wire cross-section, a related problem was considered in which the wires were infinitely long, running parallel to a perfectly conducting ground plane. The wire mean height h is much greater than the interwire spacing a_{ij}, where i and j denote the i^{th} and j^{th} wires. The self spacing a_{ii} is the radius of the i^{th} wire. The electric potential on the wire surfaces was then calculated for the static case in which a wire has a constant charge per unit length, q_i. For the eight wire cross-section, the electric potentials on the wire surfaces are:

$$\begin{bmatrix} \ell n\ 2h/a_{11} & \cdots & \ell n\ 2h/a_{18} \\ \vdots & & \vdots \\ \ell n\ 2h/a_{18} & \cdots & \ell n\ 2h/a_{88} \end{bmatrix} \begin{bmatrix} q_1 \\ \vdots \\ q_8 \end{bmatrix} = 2\pi\varepsilon \begin{bmatrix} V_1 \\ \vdots \\ V_8 \end{bmatrix} \qquad \text{(C-1)}$$

We now assume that the four tower leg wires numbered 1, 3, 5 and 7 will have equal charges per unit length, and the four stub wires numbered 2, 4, 6 and 8 will have equal charges per unit length. This symmetry was approximately true for the NEC computations on the detailed tower-stub model, where the currents on the four tower legs over the stubbed portion were within ±5% and ±8° of their average value, and the same degree of symmetry existed for the four stub wires. Making use of symmetry, equation (C-1) becomes

$$\begin{bmatrix} \ell n\ 2h/(a_{11}a_{13}a_{15}a_{17})^{\frac{1}{4}} & \ell n\ 2h/(a_{12}a_{14}a_{16}a_{18})^{\frac{1}{4}} \\ \ell n\ 2h/(a_{21}a_{23}a_{25}a_{27})^{\frac{1}{4}} & \ell n\ 2h/(a_{22}a_{24}a_{26}a_{28})^{\frac{1}{4}} \end{bmatrix} \begin{bmatrix} 4q_1 \\ 4q_2 \end{bmatrix} = 2\pi\varepsilon \begin{bmatrix} V_1 \\ V_2 \end{bmatrix} \qquad \text{(C-2)}$$

The similar equation for the two-wire cross-section with the same mean height above ground, h, is

$$\begin{bmatrix} \ell n\ 2h/a'_{11} & \ell n\ 2h/a'_{12} \\ \ell n\ 2h/a'_{21} & \ell n\ 2h/a'_{22} \end{bmatrix} \begin{bmatrix} q'_1 \\ q'_2 \end{bmatrix} = 2\pi\varepsilon \begin{bmatrix} V'_1 \\ V'_2 \end{bmatrix} . \qquad \text{(C-3)}$$

Because we want wire 1 of the two-wire cross-section to represent the combined effect of wires 1, 3, 5 and 7 of the eight-wire cross-section, then we will have $q'_1 = 4q_1$ and $V'_1 = V_1$, and similarly for the other wires, $q'_2 = 4q_2$ and $V'_2 = V'_2$. With these charge and potential conditions, equations (C-2) and (C-3) yield

$$a'_{11} = (a_{11}a_{13}a_{15}a_{17})^{\frac{1}{4}} \qquad \text{(C-4)}$$

$$a'_{22} = (a_{22}a_{24}a_{26}a_{28})^{\frac{1}{4}} \qquad \text{(C-5)}$$

$$a'_{12} = (a_{12}a_{14}a_{16}a_{18})^{\frac{1}{4}} = (a_{21}a_{23}a_{25}a_{27})^{\frac{1}{4}} . \qquad \text{(C-6)}$$

It can be seen that the tower body wire of the two-wire cross-section has a radius equal to the geometric mean of the four tower leg inter-wire spacings of the eight-wire cross-section, including the self spacing or radius, and similarly the stub wire of the two-wire cross-section has a radius equal to the geometric mean of the four stub inter-wire spacings. The spacing between wires of the two-wire cross-section equals the geometric mean of the spacing between a stub wire and the four leg wires, which equals the geometric mean of the spacing between a tower leg and the four stub wires on the eight wire cross-section. After substituting the known cross-section dimensions of the eight wires into equations (C-4) to (C-6), the computed dimensions of the two wires are radii of 2.38 m and 1.4 m for the tower body and stub wires, with a spacing of 6.30 m. The radius of the tower body wire is not much different from the value of 2.25 m obtained for the equivalent T tower model without a detuner. The stub spacing of 6.30 m from the axis of the tower body is not much different from the value of 6.28 m for the distance between the stub wire and tower axis in the eight-wire cross-section.

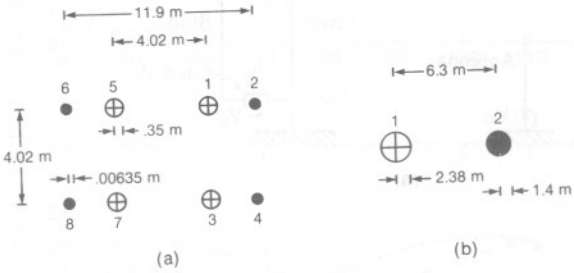

Figure 10: (a) Average cross-section of detailed tower-plus-stub model.
(b) Cross-section of simple tower-plus-stub model.
Interwire spacings and wire radii are shown.

The dimensions of the simple tower-stub model have been found. The wire radii and spacing are such that no numerical problems should occur. While equivalence between the simple tower-stub model and the detailed one has not been rigorously proven, the computed dimensions seem reasonable. The validity of the simple tower-stub model can be determined by correlation of computations with measurement.

Appendix D

Numerical Detuner Load Adjustment

The load attached to a detuner can be adjusted computationally by iteration from an initial estimate, but this procedure is inefficient, especially if one does not restrict the load impedance to be purely imaginary. A direct solution can be found by separating the power line currents into two modes. Consider the situation in Figure 11(a) in which the power line is illuminated by a source antenna and contains a load with voltage V_L across it due to its current I_L. The currents on the power line will not change if the stub load is replaced by a stub voltage source of V_L, as depicted in Figure 11(b). The power line current is the superposition of two modes, one with the antenna voltage source turned on and the stub voltage source turned off, and the other with the stub voltage source turned on and the antenna voltage source turned off. In the problem of detuner load adjustment, it is not initially known what stub load or equivalent stub voltage is required, but it is known that the total power line currents are the superposition of two modes, and that the tower base current is to be zero. Thus, the solution involves computations of current distribution on NEC for each of the two modes, with an arbitrary stub voltage source of 1 volt for example, and subsequent simple computation of the mode coefficients required to produce a total tower base current of zero. When the mode coefficients are known, the stub source voltage and total current are known, and hence the equivalent stub load, $Z_L = V_L/I_L$, can be calculated. The stub load obtained may have a large negative resistance, in which case the particular stub design is not very useful and a new design is required, assuming that it is impractical to run a coaxial cable from the transmitter to the stub load. In the stubs tested in this work, the resistance was positive or negative but

always small compared to the reactance, so it could be omitted from the load without serious deterioration of stub performance.

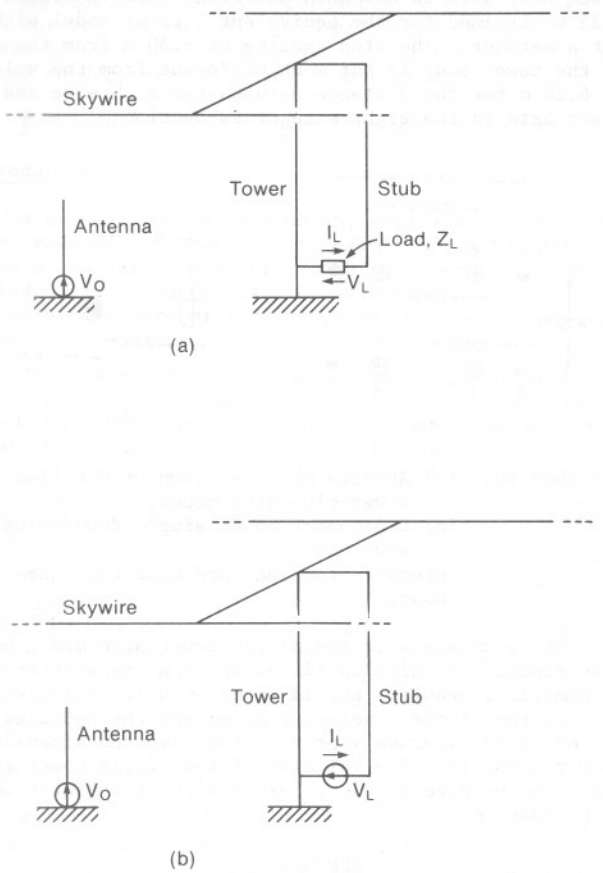

Figure 11: Antenna operating in the presence of a power line with a tower having a stub which has (a) an impedance load, and (b) an equivalent voltage source.

Acknowledgements

Ontario Hydro cooperated and assisted in the field testing. J.G. Elder designed the transmitting system and advised on measurement techniques. S.J. Kavanagh and M.M. Silva assisted in the measurements. The advice of W.V. Tilston was very useful in obtaining simplified methods. Support was provided by the Natural Sciences and Engineering Research Council of Canada, under Grants G-0362 and A-4140.

References

[1] M.M. Silva, K.G. Balmain and E.T. Ford, "Effects of Power Line Re-radiation on the Patterns of a Dual Frequency MF Antenna", IEEE Trans. Broadcasting, vol. BC-28, no.3, pp.94-103, September 1982.

[2] M.A. Tilston and K.G. Balmain, "Medium Frequency Re-radiation from an Unstrung Steel Power Line Tower", IEEE Trans. Broadcasting, vol. BC-29, no.3, pp.93-100, September 1983.

[3] K.G. Balmain, "The Effects of Re-radiation of AM Broadcast Signals", Final Report for the Communications Research Centre, Department of Communications, Ottawa, Ontario, Canada DSS Ser. No.OSU77-00288, March 1978, p.13.

[4] W. Lavrench and J.G. Dunn, reported in "The Effects of Re-radiation from Highrise Buildings, Transmission Lines, Towers and Other Structures upon AM Broadcasting Directional Arrays", Interim Report No.5, DOC Project No.4-284-15010, February 14, 1979, Ottawa, Ontario, Canada.

[5] G.D. Monteath, "Applications of the Electromagnetic Reciprocity Principle", Pergamon Press, New York, 1973.

[6] P. Knight, "Propagation Coefficient of the Beverage Aerial", Proc. IEE, vol.119, no.7, pp.821-826, July 1972.

[7] J.G. Burke and A.J. Poggio, "Numerical Electromagnetics Code (NEC) - Method of Moments", Naval Ocean Systems Centre technical document 116, July 1977.

[8] S.A. Schelkunoff and H.T. Friis, "Antennas Theory and Practice", Wiley, 1966, p.110.

[9] E.C. Jordan and K.G. Balmain, "Electromagnetic Waves and Radiating Systems", Prentice Hall, New Jersey, 1968, p.154.

[10] p. 218 in Reference [9].